Journal of Environmental Chemical Engineering 9.1 (2021): 104744

DOI: https://doi.org/10.1016/j.jece.2020.104744

Enhanced selectivity to olefins in the hydrodechlorination of trichloromethane using Ag-Pd on activated carbon catalysts

C. Fernandez-Ruiz, S. Liu, J. Bedia*, J.J. Rodriguez, L.M. Gómez-Sainero

Departamento de Ingeniería Química, Universidad Autónoma de Madrid, Cantoblanco, 28049, Madrid, Spain

**Corresponding author details:* *Telephone number: +34 91 497 29 11*
E-mail: jorge.bedia@uam.es

Abstract

Two Ag-Pd (nominal 1% wt each) bimetallic catalysts supported on commercial activated carbon were synthesized and tested, for the first time, in the hydrodechlorination (HDC) of trichloromethane (TCM) to obtain light olefins. Two different Pd precursors were used, $PdCl_2$ and $Pd(NO_3)_2$, being the resulting catalysts denoted as AgPdCl/C and AgPdN/C, respectively. A monometallic Ag catalyst was also prepared for comparison purposes. The two different Pd precursors led to different metal particle sizes and zerovalent to electrodeficient metal ratios. The monometallic Ag catalyst showed a poor dechlorination, in contrast with the bimetallic ones. AgPdN/C yielded high selectivity to paraffins, while AgPdCl/C was more selective to olefins (mostly ethylene), the desired reaction products. This better behavior of AgPdCl/C in terms of selectivity to ethylene and propylene was probably due to the existence of smaller Pd nanoparticles as monometallic sites. These Pd sites are active for the conversion of chloromethanes into light unsaturated hydrocarbons, while larger Pd clusters present higher hydrogenation ability. AgPdCl/C allowed complete TCM conversion, with high overall dechlorination and outstanding 75 % selectivity to olefins, showing very high stability at a reaction temperature of 350 °C for almost 35 h on stream. These results represent a significant improvement respect to those obtained with monometallic Pd on activated carbon catalysts reported in our previous studies. To the best of our knowledge, for the first time

it is reported such high selectivity to olefins as the above indicated from HDC of a chloromethane.

Keywords: *Hydrodechlorination; Tricloromethane; Palladium; Silver; Olefins; Paraffins.*

1. Introduction

Chloromethanes are widely used as solvents, intermediates or products in different industries. As a consequence, important amounts of these compounds are easily released to the atmosphere as a result of leaking from wastes, continuous evaporation or emissions [1–3]. Due to their health risk [4] and the role they play on atmosphere pollution, different European and worldwide regulations try to limit their release to the environment by restricting their use in industrial processes avoiding their presence on some consumables like cosmetic and foodstuffs [5–9], and applying remediation techniques. Although there are several available techniques to remove these species, only some solutions can transform them into valuable hydrocarbons, such as light paraffins and olefins. These are valuable compounds in the petrochemical industry because of their wide use as key intermediates for the manufacture of numerous products. Light olefins are mainly produced by steam and fluid-catalytic cracking [10,11], which are intensive energy-demanding processes working under severe conditions. Therefore, the development of complementary technologies is of interest. In this sense, catalytic hydrodechlorination (HDC) of chloromethanes appears as a promising way of obtaining valuable light hydrocarbons at mild conditions of pressure and temperature [12]. While the direct production of olefins can be of higher interest [13–15], most studies available obtain methane as the main reaction product of the HDC of chloromethanes. Recently, good results were reported for the dechlorination of monochloromethane in terms of selectivity to ethylene, propylene and butylene, using zeolite catalysts [16–19]. Nevertheless, those catalysts were only stable for the first few hours, hereafter, activity dropped rapidly because of coke deposition and changes of surface acidity. In previous studies of our group [13,20], significant values of selectivity to olefins were obtained with Pd based catalysts in the HDC of TCM, though they require to be improved. In contrast, as the process is simplified because coupling of two molecules is not necessary, a wide diversity of studies concerning the selective production of olefins from C2 chlorinated hydrocarbons can be found in the bibliography [21-30]. Regardless the reactant investigated, HDC studies focused on improving the selectivity to light olefins have commonly used noble or transition metals, like Pd and Ni, as active phases, due to their well-known hydrogenation ability, as well as supports of different nature, such as zeolites, metal organic frameworks and carbon materials [13,20–22,33]. However, Ni-based catalysts are prone to coke formation leading to rapid deactivation.

An interesting approach to modulate the selectivity of the HDC reaction is the use of bimetallic catalysts looking for synergistic effects. Among them, the most commonly studied are based on Pd-Pt [25,26,34,35]. Kovalchuk and d'Itri [26] postulated that bimetallic Pd-Pt catalysts are interesting for the HDC of chlorocarbons, since one metal promotes the dechlorination reaction while the other modifies the reactivity shifting the reaction towards the formation of olefins. Bimetallic catalysts try to combine the advantages of both active phases. Pd has shown a higher selectivity to C_{1+} alkanes, such as ethane and propane, and, under certain reaction conditions, high selectivity to unsaturated hydrocarbons [35,36]. Meanwhile Pt-based catalysts usually present higher resistance to deactivation by carbon deposition or chlorine adsorption [25,35,37]. The combination with other secondary active phases, such as Cu, Ag, Fe and Co, has shown significant improvements on the selectivity distribution, mainly for the HDC of C2 chlorinated hydrocarbons [23,24,27–32,38–40], besides a cost reduction. Job et al. [40] studied Pd-Ag bimetallic catalysts supported on a porous carbon xerogel in the HDC of 1,2-dichloroethane. They observed that the presence of Ag significantly increased the selectivity to ethylene compared with monometallic Pd catalyst. This increase was more significant at higher temperatures, reaching 100 % selectivity to ethylene at 250 °C, although with relatively low activity (maximum conversion of 1,2-dichloroethane of 40 % at 350 °C). Sun et al. [31] obtained 94.6% selectivity to ethylene in the hydrodechlorination of 1,2-dichloroethane at 250 °C, also with a Pd-Ag catalyst but supported on γ-Al_2O_3. In this case, the catalyst showed poor stability, and only 5% conversion was maintained after 40 hours on stream. Han et al. [32] reported high selectivity to ethylene (94 %) for the HDC of 1,2 dichloroethane after 40 h with a Pd-Ag catalyst supported on Al_2O_3, and slightly better results using Ag-Pd on ZrO_2 [41]. Despite the high selectivities obtained in these studies, none of them reported high conversion of the chlorinated reactant, which in all cases was 1,2-dichloroethane, a widely used chlorinated hydrocarbon, but less than chloromethanes. Most of the studies ascribe the good performance of Pd-Ag catalyst to the ability of forming small isolated Pd active sites, centers that we also found to promote the production of olefins from TCM HDC. There are very few reported works with this kind of bimetallic catalysts aimed to address high selectivity to olefins from trichloromethane and particularly none using Pd-Ag bimetallic catalysts.

The interest of this contribution is related with three main aspects: (i) the higher industrial importance of olefins versus other hydrocarbons commonly obtained from the HDC of chloromethanes; (ii) the suitable properties showed by Ag in order to modify the performance of Pd towards the formation of olefins in other hydrodechlorination reactions and (iii) the absence of studies devoted to the production of olefins from the HDC of trichloromethane. Therefore, the present study is focused on the synthesis and characterization of Ag-Pd catalysts supported on activated carbon and their application to produce selectively light olefins from the HDC of trichloromethane, reaching a value not yet reported in the literature to the best of our knowledge.

2. Experimental procedure

2.1. Materials and chemicals

A commercial activated carbon was used as support, as received from Merck. $PdCl_2$ (>99 %), $Pd(NO_3)_2$ and $AgNO_3$ ($\geq$99%) were supplied by Sigma-Aldrich, and HCl (37.5 %) by Panreac. Trichoromethane (0.4 % mol in N_2), H_2 and N_2 (both 99.999 % purity) were provided by Praxair.

2.2. Synthesis of the catalysts

The Ag monometallic catalyst was prepared by incipient wetness impregnation of the activated carbon with $AgNO_3$ aqueous solution to obtain 1.0 % of Ag in weight. The solid was then dried for 24 h at 70 °C in an oven. In the case of bimetallic catalysts, the support was firstly impregnated with $AgNO_3$ and dried as abovementioned. Then, Pd was incorporated by incipient wetness impregnation with $PdCl_2$ or $Pd(NO_3)_2$ in HCl aqueous solutions (1 M), to obtain also a nominal 1 %wt. Pd, and the resulting solid dried again for 24 h at 70 °C. The catalysts were denoted as Ag/C, AgPdCl/C and AgPdN/C, corresponding to, respectively, monometallic Ag and bimetallic Ag-Pd prepared with $Pd(NO_3)_2$ and $PdCl_2$ as palladium precursors,

2.3. Characterization

Before every characterization study, the catalysts were reduced under continuous H_2 flow (50 $Ncm^3 \cdot min^{-1}$) at 250 °C for 2 h, in order to analyse them under the operating conditions of the hydrodechlorination experiments. The porous texture was assessed by

N_2 adsorption-desorption at -196 °C in a Tristar II 3020 equipment (Micromeritics). The samples were previously degassed for 12 h at 150 °C until residual pressure of $5 \cdot 10^{-3}$ Torr with a VacPrep 061 equipment (Micromeritics). The specific surface area (A_{BET}) was calculated from the BET equation [42]. The micropore volume (V_{micro}) and the external or non-microporous surface area (A_{ext}) were obtained by the t-method [43]. The total pore volume was estimated from the amount of N_2 adsorbed at $P/P_o \approx 0.99$ converted to liquid volume (V_{pore}). The bulk content of Ag and Pd present on the catalysts was quantified by total reflection of X-ray fluorescence (TXRF), with a Bruker S2 PICOFOX apparatus, operated at 50 kV and 600 μA. The X-ray diffraction (XRD) patterns of the catalysts were obtained with a X'pert PRO PANalytical diffractometer. The powdered samples were scanned using a CuKα monochromatic radiation of $\lambda = 0.15406$ nm and a Ge monofilter. The scanning range of $2\theta = 20\text{-}90^o$ was obtained with a scan step size of 0.020^o using a collection time of 5 s. X-ray photoelectron spectroscopy (XPS) was performed to analyse the external surface composition of the reduced catalysts with a Thermo Scientific equipment with Al Kα radiation (1486.7 eV). The general spectra of the samples were recorded by scanning binding energy (BE) from 0 to 1200 eV. C 1s peak at 284.5 eV was taken as an internal standard to correct the changes in BE caused by sample charging. The deconvolution was performed using smooth Shirley background and mixed Gaussian–Lorentzian functions fitting by a least-squares method. The morphologies and mean particle size of the metallic particles (Pd and Ag) were analyzed by transmission electron microscopy (TEM). All the micrographs were acquired with a JEM 2100 microscope (JEOL, Akishima, Tokyo, Japan) with an accelerating voltage of 200 kV. More than 100 particles were measured for the calculation of the mean particle size.

2.4. Gas-phase HDC experiments

The HDC experiments were carried out in a continuous flow reaction system (Micro-Activity by PID) described in more detail elsewhere [36], using a quartz fixed bed microreactor (4 mm internal diameter). The catalysts were reduced "in situ" under a H_2 flow (50 $Ncm^3 \cdot min^{-1}$) at 250 °C for 2 h. The runs were conducted at atmospheric pressure, inlet total flow rate (TCM+H_2+N_2) of 100 $Ncm^3 \cdot min^{-1}$ with trichloromethane (TCM) concentration of 1000 ppmv and H_2/TCM molar ratio of 100:1. The catalyst weight was 0.213 g, resulting in a space time of 0.8 $kgcat \cdot h \cdot mol^{-1}$ TCM. The reaction temperatures

tested covered the range 125 to 400 ºC. A gas chromatograph (Varian 450-GC) was coupled at the exit of the reaction system, equipped with a capillary column (Varian, CP-SilicaPLOT, 60 m) and a flame ionization detector (FID).

3. Results and discussion

3.1. Characterization of the catalysts

Figure 1 represents the N_2 adsorption-desorption isotherms at -196 °C of the activated carbon used as support (Carbon Merck) and the catalysts. All of them show a similar shape associated to the activated carbon support, characteristic of microporous materials with some contribution of mesoporosity, as revealed by the smooth slope of the horizontal-like branch and the presence of a small hysteresis loop in all cases. The knee of the curves suggests a relatively wide distribution of micropores size. Some small decrease of the amount adsorbed can be observed in the catalysts respect to the bare support, indicative of low-significance pore blockage by the deposited metallic phase. **Table 1** summarizes the textural characteristics of these materials, showing BET surface area and pore volume values typical of activated carbons, with most of the surface area corresponding to micropores and somewhat more than 10 % belonging to the so-called external or non-microporous area. These characteristics are quite similar to the previously reported for other activated carbon-supported Pd catalysts [44,45]. It is worth to mention that AgPdN/C catalyst yielded the lowest A_{BET} and V_{micro} values, probably due to larger metal particles associated to the use of nitrate as Pd precursor. It has been reported that $PdCl_2$ leads to metal particles with higher dispersion than $Pd(NO_3)_2$, due to the stronger interaction of this last with the activated carbon surface [46,47].

Figure 1

Table 1

Figure 2 shows the XRD patterns of the three reduced catalysts, where it can be clearly observed the presence of two broad peaks centered at around 26.7 and 44.4°,

typical of turbostratic carbon materials. The pattern of Ag/C shows peaks at around 38.1, 44.4, 64.4, 77.4 and 81.5° corresponding to (111), (200), (220), (311) and (222) planes of fcc metallic silver (JCPDS No.04-0783) [48,49], which can be also observed in AgPdCl/C and AgPdN/C spectra, although with much lower intensity. The higher intensity of these peaks in the monometallic Ag catalysts indicates a higher crystallinity of the Ag particles in this sample. The mean size of these Ag particles, calculated by applying the Scherrer equation to the (111) peak, was found to be 78.8, 56.6 and 43.5 nm for Ag, AgPdCl/C and AgPdN/C catalysts, respectively. Despite the method and precursor used for introducing Ag is the same for all the catalysts, clear differences can be observed in both dispersion and distribution of Ag particles. This can be explained by the dissolution and redispersion of metallic particles as a consequence of the later use of acid solutions (1 M) to dissolve the palladium precursor salts. The appearance of a new diffraction peak on AgPdN/C catalyst of lower crystallinity, adjacent to Ag (111), can be due to the presence of crystallites composed by Ag and Pd, bimetallic Ag-Pd particles [50,51]. The presence of AgCl cannot either be discarded since the AgPdCl/C pattern shows clearly diffraction peaks at around 27.8, 32.2, 46.2, 54.8º that can be associated to (111), (200), (220) and (311) planes of AgCl crystals respectively (JCPDS No. 31-1238) [48]. The incorporation of Pd resulted in the appearance of new peaks in the XRD patterns. AgPdN/C diffraction pattern show low intensity peaks at around 40.0, 46.7, 68.1 and 82.1º corresponding to the (111), (200), (220), and (311) atomic planes of fcc Pd (JCPDS No. 87-0641) [52]. The peak corresponding to the (200) plane at around 46.7º is not clearly observed because it is partially masked by the broad peak at 44.0º of the amorphous carbon support. The observation of these peaks in AgPdN/C catalyst indicates that Pd crystals are of relatively large size. The mean particle size, obtained by Scherrer equation, resulted to be 26.2 nm. These peaks associated to metallic Pd are not observed in the XRD pattern of AgPdCl/C catalyst, suggesting a high dispersion and consequently a lower palladium crystal sizes due to the utilization of $PdCl_2$ precursor in the synthesis of this catalyst [46].

Figure 2

Figure 3 shows representative TEM images beside to the mean metal particle size of the different catalysts. Metal particles with spherical shape and different sizes can be

clearly observed for the different catalysts. In the case of monometallic silver catalysts, AgC, big silver particles are observed, with a mean size of 58.4 nm. Lower metal particles sizes are observed for the two palladium monometallic and bimetallic catalysts. However, bimetallic catalysts show an intermediate metal particles size, with values between the monometallic ones prepared from the same precursor, namely, 1.8, 3.6, 10.7 and 17.8 nm for PdCl/C, AgPdCl/C, PdN/C and AgPdN/C, respectively. It can be concluded that Ag nanoparticles are in general trend of bigger size, although the Pd deposition seems to produce a reduction of the Ag particles sizes, besides to well-dispersed Pd particles. The use of $PdCl_2$ as palladium precursor results in a significantly lower particle size than the use of $Pd(NO_3)_2$. These results agree well with the XRD observations.

Figure 3

Table 2 includes the Ag and Pd bulk content of the catalysts. The contents are close to the nominal 1.0%, with general deviations lower or equal to 10%, which confirms the proper deposition of the metals during the synthesis stage. **Table 2** also summarizes the surface concentration of Ag and Pd on the catalysts, and the relative contribution of zerovalent and electrodeficient metallic species as obtained by deconvolution of their corresponding XPS profiles (**Figures 4 and 5**). Ag/C, PdCl/C and AgPdCl/C catalysts yielded values comparable to the nominal bulk ones, indicating a more or less homogeneous distribution, while in the case of the PdN/C and AgPdN/C catalysts egg-shell distributions of both metallic phases can be inferred, particularly accused for Pd. The Ag3d XPS of **Figure 4** shows the doublet corresponding to Ag $3d_{5/2}$ and $3d_{3/2}$ contributions separated by 6.0 eV [53,54]. Deconvolution of the Ag $3d_{5/2}$ signal of the bimetallic catalysts gives two contributions one located at around 368.2 eV, and the other at approximately 367.5 eV, related to the presence of Ag^0 and Ag^{n+}, respectively [55]. The monometallic Ag catalyst showed only the zerovalent species. AgPdCl/C shows a small contribution of Ag^{n+} while AgPdN/C contains Ag mainly in electrodeficient state. The presence of Ag^{n+} in the bimetallic catalysts can be explained by the charge redistribution between metallic Ag and Pd, because of the higher electronegativity of Pd respect to Ag [56–58]. It is mainly observed in AgPdN/C because of the significant higher amount of surface metallic species in this sample. The higher concentration of Ag and Pd

on the AgPdN/C surface (1.8 and 7.5 %, respectively) in comparison with AgPdCl/C (0.8 and 0.9 %, respectively) would favor the contact between both active phases, promoting the formation of AgPd bimetallic particles. **Figure 5** represents the Pd 3d XPS profiles of the Pd-containing catalysts. Those spectra can be deconvoluted on the basis of doublets corresponding to Pd $3d_{5/2}$ and $3d_{3/2}$, separated by 5.3 eV, due to the spin orbital splitting [55]. The Pd $3d_{5/2}$ peak of the metallic palladium signal (Pd^0) is located at around 335.5 eV, while that of electrodeficient palladium (Pd^{n+}) is close to 338.0 eV. The catalysts from the $Pd(NO_3)_2$ salt, AgPdN/C and PdN/C, showed a higher proportion of Pd^0 than those from $PdCl_2$, AgPdCl/C and PdCl/C (**Table 2**), which is in agreement with other results reported in the literature concluding that Pd nitrate gives higher proportion of zerovalent Pd species than chloride [59,60]. Álvarez-Montero et al. [60] observed that an acid solution of Pd chloride precursor, as in the case of $PdCl_2$ solution, strongly interacts with the activated carbon surface, leading to the formation of small Pd particles, homogeneously distributed in the pores of the catalysts. In contrast, $Pd(NO_3)_2$ interaction with the carbon surface seems to be weaker, favoring aggregation with other Pd particles, thus decreasing Pd dispersion [46,47,61]. On the other hand, AgPdCl/C catalyst shows higher Pd^0 proportion (71 %) than that of previously reported for monometallic Pd catalyst supported on the same activated carbon (57 %) [62]. This higher concentration of zerovalent Pd in AgPdCl/C can be due to electronic transference from Ag sites to Pd because of the higher electronegativity of the latter.

Figure 4

Figure 5

Table 2

3.2. HDC results

Figure 6 depicts the TCM conversion at different temperatures with the two catalysts tested and the two monometallic PdCl/C and PdN/C ones, which have been included for comparison purposes. The monometallic Ag catalyst showed low

dechlorination ability and suffered a very rapid deactivation even at low reaction temperatures. Moreover, a quite significant carbon imbalance was observed (around 50%), suggesting the formation and deposition of condensation oligomeric species, that could block the Ag active sites. In contrast, both Pd monometallic and Ag-Pd bimetallic catalysts allowed complete TCM conversion at temperatures beyond 175-200 ºC, with high overall dechlorination, which is almost complete above 300 ºC. These results are quite similar to the obtained in our previous studies with monometallic Pd catalysts supported on activated carbon under the same working conditions [12,20]. Besides, the current catalysts showed slightly higher conversion than those reported by other authors on the HDC of tetrachloromethane (TTCM) with AgPd-based catalysts at low temperatures (125 ºC) [30,63]. According to the literature, Ag is able to adsorb TCM and to break C-Cl bonds, while Pd in the vicinity promotes dissociative chemisorption of H_2, providing H atoms to the Ag sites [30,64].

Figure 6

Figure 7 shows the selectivity to the different reaction products from the experiments of **Figure 6** with the AgPdN/C, AgPdCl/C, PdN/C and PdCl/C catalysts. The reaction products were methane, other light alkanes (ethane and propane) and light olefins (ethylene and propylene), besides the resulting from incomplete dechlorination of TCM, namely, monochloromethane (MCM) and dichloromethane (DCM) (difference up to 100% in the Figure). The catalysts allowed a high dechlorination, which increases with reaction temperature, but significant differences can be observed between them. As a general trend, the selectivity to olefins increases at increasing temperature but the AgPdCl/C is much more selective to those reaction products, which are the objective of our work. Above 250 ºC, this catalyst describes a dramatic increase of the selectivity to ethylene plus propylene, reaching 76 % at 350 ºC with 100 % TCM conversion and almost complete overall dechlorination. The addition of Ag to Pd catalysts was found to enhance the selectivity to ethylene in the hydrodechlorination of 1,2-dichloroethane [40,65]. However, it has been reported that larger Pd clusters favor the hydrogenation of unsaturated hydrocarbons, while lower sized Pd clusters facilitate their desorption, thus increasing the selectivity to olefins [32,38,40,66]. As indicated before, the mean size of

metal particles in the AgPdN/C and AgPdCl/C catalysts were 17.8 and 3.6 nm, respectively. Formation of larger Pd clusters is more likely as the concentration of Pd on the catalyst surface is higher. That is the case of AgPdN/C, in contrast with AgPdCl/C (see **Table 2**). In addition, AgPdN/C also yielded higher Ag^{+}/Ag^{0} and lower Pd^{n+}/Pd^{0} ratios, suggesting a higher interaction between Ag and Pd, which denotes that they are closer to each other. This limits the existence of single Pd sites. On the contrary, the presence of single Pd nanoparticles deposited on AgPdCl/C surface appears to be significant. The selectivities to olefins obtained with AgPdCl/C improve considerably compared to those obtained with monometallic Pd catalyst. We have observed in previous studies that Pd^{0} favors the formation of olefins, while Pd^{n+} leads to the formation of saturated hydrocarbons in the HDC of chloromethanes with Pd on activated carbon catalysts [12,13]. The high proportion of Pd^{0} (71%, **Table 2**) combined with the low metal particle size (3.6 nm, **Figure 3**) of AgPdCl/C justify the higher selectivities to olefins achieved with this catalyst. The high proportion of Ag^{0} of this catalyst compared to AgPdN/C may also influence its high selectivity to olefins.

As indicated before, with both bimetallic catalysts higher temperatures within the range tested favored overall dechlorination, in addition to the higher selectivity to olefins In that respect, AgPdN/C behaved somewhat better than AgPdCl/C, but this last gave also fairly good results, with complete conversion of TCM and selectivities to chlorinated byproducts (MCM and DCM) around 5 % at 300 ºC and almost negligible at 400 ºC (see Figure 6). However, these high temperatures usually affect to the carbon unbalance, which was in every case lower than 20 %, probably provoked by the production of condensation products at 350 °C. This can limit the stability of the catalysts by deactivating them in long-term experiments.

Figure 7

The long-term stability of the AgPdCl/C catalyst was tested, and the results can be seen in **Figure 8**, where the evolution of TCM conversion and the selectivities to the reaction products upon time on stream at 350 °C are presented. The catalyst maintained quite stable TCM conversion, close to 100 % for almost 35 h and afterwards a rapid

deactivation was observed up to what appears some residual activity of no more than 20 %. However, the selectivities to the different lumps of reaction products remained almost unchanged during the whole experiment (65 h on stream). Despite that deactivation, this catalyst behaved more stable than other AgPd catalysts reported in the literature for the HDC of 1,2-dichloroethane [31,32,41] and some of the monometallic Pd on activated carbon catalysts prepared and tested by our group in the HDC of TCM [13]. The observed loss of activity while maintaining the selectivity to olefins suggests that deactivation may proceed through partial inhibition of both Pd and Ag sites. The deactivation may be due to the formation of stable chlorides and deposition of oligomeric byproducts [23,31,41] and to the inability of Pd sites to provide H atoms to the Ag sites. Meanwhile, single Pd sites are still capable of maintaining some residual HDC dechlorination into ethylene without the presence of near Ag sites.

Figure 8

Conclusions

Bimetallic AgPd catalysts prepared by incipient wetness impregnation on activated carbon showed good ability for the HDC of TCM at relatively mild temperature and ambient-like pressure. The use of $PdCl_2$ and $Pd(NO_3)_2$ as Pd precursors gave rise to different surface concentrations of Pd and Ag as well as ratios of zerovalent to electrodefficient metallic species and metal particles sizes. $Pd(NO_3)_2$ led to larger Pd particles than those obtained from $PdCl_2$ due to the different interactions with the carbon support. The monometallic Ag catalyst showed significantly lower TCM conversion, with higher relative proportions of chlorinated species (DCM and MCM) among the reaction products in addition to very rapid deactivation. In the absence of Pd, dissociative chemisorption of H_2 does not take place and therefore atomic hydrogen is not provided to Ag sites. In contrast, both AgPd bimetallic catalysts allowed closely high TCM conversions, up to almost 100 % even at relatively low temperature of around 175 °C, accompanied also of very high overall dechlorination. However, the resulting selectivity distribution differed notably with both catalysts. AgPdCl/C yielded significantly higher selectivity to light olefins (ethylene and propylene), which were the objective of the

current work. That selectivity reached somewhat more than 75 % at 350 °C. This catalyst seems to present smaller well-distributed Pd particles than the AgPdN/C one, according to the XRD profiles, with most Pd as single metal sites and mainly in the zerovalent state. These are the ones promoting conversion of TCM preferably into light olefins. The synergistic behavior of AgPdCl/C bimetallic catalyst can be explained as follows: Ag sites are able to adsorb TCM and to break C-Cl bonds, while Pd sites in the vicinity can promote dissociative chemisorption of H_2, providing H atoms to the Ag sites, yielding unsaturated hydrocarbons. On the other hand, the electronic transference from Ag sites to Pd, because of the higher electronegativity of the latter, leads to a high concentration of zero-valent Pd which in addition to the small size of Pd particles inhibit further hydrogenation of olefins. In contrast, the use of palladium nitrate, led to significantly higher surface concentration of Pd with larger particle size, promoting hydrogenation, thus leading mainly to ethane and propane. AgPdCl/C showed highly stable performance upon 35 h on stream, followed by a rapid loss of activity for TCM hydrodechlorination although maintaining the high selectivity towards olefins. To the best of our knowledge, for the first time it is reported such a high selectivity to olefins as the above mentioned from HDC of trichloromethane.

Acknowledgements

Authors acknowledge financial support from FEDER/Ministerio de Ciencia, Innovación y Universidades – Agencia Estatal de Investigación/CTM2017-85498-R. C. Fernández Ruiz acknowledges MINECO for his research grant.

References

1. Sherry, D.; McCulloch, A.; Liang, Q.; Reimann, S.; Newman, P. A. Current sources of carbon tetrachloride (CCl_4) in our atmosphere. *Environ. Res. Lett.* **2018**, *13*, 024004.

2. Lourencetti, C.; Grimalt, J. O.; Marco, E.; Fernandez, P.; Font-Ribera, L.; Villanueva, C. M.; Kogevinas, M. Trihalomethanes in chlorine and bromine disinfected swimming pools: Air-water distributions and human exposure. *Environ. Int.* **2012**, *45*, 59–67.

3. Chen, W.-H.; Chen, Z.-B.; Yuan, C.-S.; Hung, C.-H.; Ning, S.-K. Investigating the

differences between receptor and dispersion modeling for concentration prediction and health risk assessment of volatile organic compounds from petrochemical industrial complexes. *J. Environ. Manage.* **2016**, *166*, 440–449.

4. Tsai, W.-T. Fate of Chloromethanes in the Atmospheric Environment: Implications for Human Health, Ozone Formation and Depletion, and Global Warming Impacts. *Toxics* **2017**, *5*, 23.

5. European Union DIRECTIVE 2009/32/EC of the European Parliament and of the Council of 23 April 2009 on the approximation of the laws of the Member States on extraction solvents used in the production of foodstuffs and food ingredients. *Off. J. Eur. Union* **2009**.

6. European Union Council Decision 455/2009/EC amending Council Directive 76/769/EEC as regards restrictions on the marketing and use of dichloromethane. *Off. J. Eur. Union* **2009**, *L137*, 136–148.

7. The European Parliament and the council of The European Union Regulation (EC) No 1223/2009 of the European Parliament and of the Council of 30 November 2009 on cosmetic products. *Off. J. Eur. Union* **2009**.

8. The European Parliament and the council of The European Union Directive 2013/39/EU of the European Parliament and of the Council of 12 August 2013 amending Directives 2000/60/EC and 2008/105/EC as regards priority substances in the field of water policy. *Off. J. Eur. Union* **2013**.

9. European Commission Commission Directive (EU) 2017/164 of 31 January 2017 establishing a fourth list of indicative occupational exposure limit values. *Off. J. Eur. Union* **2017**.

10. Sadrameli, S. M. Thermal/catalytic cracking of hydrocarbons for the production of olefins: A state-of-the-art review I: Thermal cracking review. *Fuel* **2016**, *173*, 285–297.

11. Sadrameli, S. M. Thermal/catalytic cracking of liquid hydrocarbons for the production of olefins: A state-of-the-art review II: Catalytic cracking review. *Fuel* **2016**, *173*, 285–297.

12. Fernandez-Ruiz, C.; Bedia, J.; Bonal, P.; Rodriguez, J. J.; Gómez-Sainero, L. M. Chloroform conversion into ethane and propane by catalytic hydrodechlorination with

Pd supported on activated carbons from lignin. *Catal. Sci. Technol.* **2018**, *8*, 3926–3935.

13. Fernandez-Ruiz, C.; Bedia, J.; Andreoli, S.; Eser, S.; Rodriguez, J. J.; Gómez-Sainero, L. M. Selectivity to Olefins in the Hydrodechlorination of Chloroform with Activated Carbon-Supported Palladium Catalysts. *Ind. Eng. Chem. Res.* **2019**, *58*, 20592–20600.

14. McFarland, E. Unconventional Chemistry for Unconventional Natural Gas. *Science (80-.).* **2012**, *338*, 340–342.

15. Paunovic, V.; Zichittella, G.; Moser, M.; Amrute, A. P.; Pérez-Ramírez, J. Catalyst design for natural-gas upgrading through oxybromination chemistry. *Nat. Chem.* **2016**, *8*, 803–809.

16. Jiang, Z.; Shen, B. X.; Zhao, J. G.; Wang, L.; Kong, L. T.; Xiao, W. G. Enhancement of Catalytic Performances for the Conversion of Chloromethane to Light Olefins over SAPO-34 by Modification with Metal Chloride. *Ind. Eng. Chem. Res.* **2015**, *54*, 12293–12302.

17. Kong, L.; Shen, B.; Jiang, Z.; Zhao, J.; Liu, J. Synthesis of SAPO-34 with the presence of additives and their catalytic performance in the transformation of chloromethane to olefins. *React. Kinet. Mech. Catal.* **2015**, *114*, 697–710.

18. Wang, T.; Yang, C.; Li, S.; Yu, G.; Liu, Z.; Wang, H.; Gao, P.; Sun, Y. Solvent-Free Synthesis of Mg-Incorporated Nanocrystalline SAPO-34 Zeolites via Natural Clay for Chloromethane-to-Olefin Conversion. *ACS Sustain. Chem. Eng.* **2020**, *8*, 4185–4193.

19. Shin, Y. H.; Kweon, S.; Park, M. B.; Chae, H. J. Comparative study of CHA- and AEI-type zeolytic catalysts for the conversion of chloromethane into light olefins. *Korean J. Chem. Eng.* **2018**, *35*, 1433–1440.

20. Fernandez-Ruiz, C.; Bedia, J.; Grau, J. M.; Romero, A. C.; Rodríguez, D.; Rodríguez, J. J.; Gómez-Sainero, L. M. Promoting Light Hydrocarbons Yield by Catalytic Hydrodechlorination of Residual Chloromethanes Using Palladium Supported on Zeolite Catalysts. *Catalysts* **2020**, *10*, 199.

21. Baran, R.; Kamińska, I. I.; Śrębowata, A.; Dzwigaj, S. Selective hydrodechlorination of 1,2-dichloroethane on NiSiBEA zeolite catalyst: Influence of the

preparation procedure on a high dispersion of Ni centers. *Microporous Mesoporous Mater.* **2013**, *169*, 120–127.

22. Ning, X.; Sun, Y.; Fu, H.; Qu, X.; Xu, Z.; Zheng, S. N-doped porous carbon supported Ni catalysts derived from modified Ni-MOF-74 for highly effective and selective catalytic hydrodechlorination of 1,2-dichloroethane to ethylene. *Chemosphere* **2020**, *241*, 124978.

23. Pirard, S. L.; Pirard, J. P.; Heyen, G.; Schoebrechts, J. P.; Heinrichs, B. Experimental procedure and statistical data treatment for the kinetic study of selective hydrodechlorination of 1,2-dichloroethane into ethylene over a Pd-Ag sol-gel catalyst. *Chem. Eng. J.* **2011**, *173*, 801–812.

24. Rhodes, W. D.; Kovalchuk, V. I.; McDonald, M. A. Reaction pathways of halocarbon catalytic oligomerization. *Catal. Commun.* **2012**, *18*, 98–101.

25. Granados-Fócil, A. A.; Núñez-Correa, S.; Martín-Guaregua, N. C.; García-Mendoza, C.; Woolfolk-Frías, L. G.; De Los Reyes-Heredia, J. A. Characterization of Highly Active Al_2O_3 -TiO_2 Supported Pt and Pd Catalysts for Hydrodechlorination of 1,2-Dichloroethane. *Int. J. Chem. React. Eng.* **2019**, *17*, 1–10.

26. Kovalchuk, V. I.; D'Itri, J. L. Catalytic chemistry of chloro- and chlorofluorocarbon dehalogenation: From macroscopic observations to molecular level understanding. *Appl. Catal. A Gen.* **2004**, *271*, 13–25.

27. Srębowata, A.; Lisowski, W.; Sobczak, J. W.; Karpinski, Z. Hydrogen-assisted dechlorination of 1,2-dichloroethane on active carbon supported palladium-copper catalysts. *Catal. Today* **2011**, *175*, 576–584.

28. Meshesha, B. T.; Barrabés, N.; Llorca, J.; Dafinov, A.; Medina, F.; Föttinger, K. PdCu alloy nanoparticles on alumina as selective catalysts for trichloroethylene hydrodechlorination to ethylene. *Appl. Catal. A Gen.* **2013**, *453*, 130–141.

29. Han, Y.; Zhou, J.; Wang, W.; Wan, H.; Xu, Z.; Zheng, S.; Zhu, D. Enhanced selective hydrodechlorination of 1,2-dichloroethane to ethylene on Pt–Ag/TiO_2 catalysts prepared by sequential photodeposition. *Appl. Catal. B Environ.* **2012**, *125*, 172–179.

30. Lu, M.; Sun, J.; Zhang, D.; Li, M.; Zhu, J.; Shan, Y. Highly selective hydrodechlorination of CCl_4 into $CHCl_3$ on Ag–Pd/carbon catalysts. *React. Kinet.*

Mech. Catal. **2010**, *100*, 99–103.

31. Sun, J.; Han, Y.; Fu, H.; Wan, H.; Xu, Z.; Zheng, S. Selective hydrodechlorination of 1,2-dichloroethane catalyzed by trace Pd decorated Ag/Al_2O_3 catalysts prepared by galvanic replacement. *Appl. Surf. Sci.* **2018**, *428*, 703–709.

32. Han, Y.; Gu, G.; Sun, J.; Wang, W.; Wan, H.; Xu, Z.; Zheng, S. Selective hydrodechlorination of 1,2-dichloroethane to ethylene over $Pd\text{-}Ag/Al_2O_3$ catalysts prepared by surface reduction. *Appl. Surf. Sci.* **2015**, *355*, 183–190.

33. Śrębowata, A.; Baran, R.; Łomot, D.; Lisovytskiy, D.; Onfroy, T.; Dzwigaj, S. Remarkable effect of postsynthesis preparation procedures on catalytic properties of Ni-loaded BEA zeolites in hydrodechlorination of 1,2-dichloroethane. *Appl. Catal. B Environ.* **2014**, *147*, 208–220.

34. Bedia, J.; Gómez-sainero, L. M.; Grau, J. M.; Busto, M.; Martin-martinez, M.; Rodriguez, J. J. Hydrodechlorination of dichloromethane with mono- and bimetallic Pd – Pt on sulfated and tungstated zirconia catalysts. *J. Catal.* **2012**, *294*, 207–215.

35. Bonarowska, M.; Śrębowata, A.; Karpiński, Z. Synergistic effects in hydrodechlorination of organic compounds catalyzed by metals. *Ann. UMCS, Chem.* **2010**, *65*, 1–8.

36. Gómez-Sainero, L. M.; Palomar, J.; Omar, S.; Fernández, C.; Bedia, J.; Álvarez-Montero, A.; Rodriguez, J. J. Valorization of chloromethanes by hydrodechlorination with metallic catalysts. *Catal. Today* **2018**, *310*, 75–85.

37. Álvarez-Montero, M. A.; Gómez-Sainero, L. M.; Mayoral, A.; Diaz, I.; Baker, R. T.; Rodriguez, J. J. Hydrodechlorination of chloromethanes with a highly stable Pt on activated carbon catalyst. *J. Catal.* **2011**, *279*, 389–396.

38. Ball, M. R.; Rivera-Dones, K. R.; Stangland, E.; Mavrikakis, M.; Dumesic, J. A. Hydrodechlorination of 1,2-dichloroethane on supported AgPd catalysts. *J. Catal.* **2019**, *370*, 241–250.

39. Kulkarni, P. P.; Kovalchuk, V. I.; D'Itri, J. L. Oligomerization pathways of dichlorodifluoromethane hydrodechlorination catalyzed by activated carbon supported Pt-Cu, Pt-Ag, Pt-Fe, and Pt-Co. *Appl. Catal. B Environ.* **2002**, *36*, 299–309.

40. Job, N.; Heinrichs, B.; Ferauche, F.; Noville, F.; Marien, J.; Pirard, J.-P. Hydrodechlorination of 1,2-dichloroethane on Pd–Ag catalysts supported on tailored texture carbon xerogels. *Catal. Today* **2005**, *102–103*, 234–241.

41. Han, Y.; Sun, J.; Fu, H.; Qu, X.; Wan, H.; Xu, Z.; Zheng, S. Highly selective hydrodechlorination of 1,2-dichloroethane to ethylene over Ag-Pd/ZrO_2 catalysts with trace Pd. *Appl. Catal. A Gen.* **2016**, *519*, 1–6.

42. Brunauer, S.; Emmett, P. H.; Teller, E. Adsorption of Gases in Multimolecular Layers. *J. Am. Chem. Soc.* **1938**, *60*, 309–319.

43. Lippens, B. Studies on pore systems in catalysts V. The t method. *J. Catal.* **1965**, *4*, 319–323.

44. Duarte, F.; Maldonado-Hódar, F. J.; Madeira, L. M. Influence of the characteristics of carbon materials on their behaviour as heterogeneous Fenton catalysts for the elimination of the azo dye Orange II from aqueous solutions. *Appl. Catal. B Environ.* **2011**, *103*, 109–115.

45. Arevalo-Bastante, A.; Álvarez-Montero, M. A.; Bedia, J.; Gómez-Sainero, L. M.; Rodriguez, J. J. Gas-phase hydrodechlorination of mixtures of chloromethanes with activated carbon-supported platinum catalysts. *Appl. Catal. B Environ.* **2015**, *179*, 551–557.

46. Zhang, X.; Du, Y.; Jiang, H.; Liu, Y.; Chen, R. Matching Relationship Between Carbon Material and Pd Precursor. *Catal. Letters* **2019**, *149*, 813–822.

47. Gopinath, R.; Seshu Babu, N.; Vinod Kumar, J.; Lingaiah, N.; Sai Prasad, P. S. Influence of Pd precursor and method of preparation on hydrodechlorination activity of alumina supported palladium catalysts. *Catal. Letters* **2008**, *120*, 312–319.

48. Wang, H.; Yang, X.; Zi, J.; Zhou, M.; Ye, Z.; Li, J.; Guan, Q.; Lv, P.; Huo, P.; Yan, Y. High photocatalytic degradation of tetracycline under visible light with Ag/AgCl/activated carbon composite plasmonic photocatalyst. *J. Ind. Eng. Chem.* **2016**, *35*, 83–92.

49. Çelik Kazici, H.; Yildiz, F.; İzgi, M. S.; Ulaş, B.; Kivrak, H. Novel activated carbon supported trimetallic PdCoAg nanoparticles as efficient catalysts for the hydrolytic dehydrogenation of ammonia borane. *Int. J. Hydrogen Energy* **2019**, *44*, 10561–10572.

50. Holade, Y.; Morais, C.; Arrii-Clacens, S.; Servat, K.; Napporn, T. W.; Kokoh, K. B. New Preparation of PdNi/C and PdAg/C Nanocatalysts for Glycerol Electrooxidation in Alkaline Medium. *Electrocatalysis* **2013**, *4*, 167–178.

51. Satyanarayana, M.; Rajeshkhanna, G.; Sahoo, M. K.; Rao, G. R. Electrocatalytic Activity of $Pd_{20-x}Ag_x$ Nanoparticles Embedded in Carbon Nanotubes for Methanol Oxidation in Alkaline Media. *ACS Appl. Energy Mater.* **2018**, *1*, 3763–3770.

52. Zhou, J.; Lou, Z.; Yang, K.; Xu, J.; Li, Y.; Liu, Y.; Baig, S. A.; Xu, X. Electrocatalytic dechlorination of 2,4-dichlorobenzoic acid using different carbon-supported palladium moveable catalysts: Adsorption and dechlorination activity. *Appl. Catal. B Environ.* **2019**, *244*, 215–224.

53. Herrmann, J. M.; Disdier, J.; Pichat, P. Photocatalytic deposition of silver on powder titania: Consequences for the recovery of silver. *J. Catal.* **1988**, *113*, 72–81.

54. Arabatzis, I. M.; Stergiopoulos, T.; Bernard, M. C.; Labou, D.; Neophytides, S. G.; Falaras, P. Silver-modified titanium dioxide thin films for efficient photodegradation of methyl orange. *Appl. Catal. B Environ.* **2003**, *42*, 187–201.

55. Moulder, J. F.; Stickle, W. F.; Sobol, P. E.; Bomben, K. D. *Handbook of X-ray photoelectron spectroscopy: a reference book of standard spectra for identification and interpretation of XPS data*; 1992.

56. Xia, X.; Wang, Y.; Ruditskiy, A.; Xia, Y. 25th Anniversary Article: Galvanic Replacement: A Simple and Versatile Route to Hollow Nanostructures with Tunable and Well-Controlled Properties. *Adv. Mater.* **2013**, *25*, 6313–6333.

57. Olovsson, W.; Bech, L.; Andersen, T. H.; Li, Z.; Hoffmann, S. V.; Johansson, B.; Abrikosov, I. A.; Onsgaard, J. Core-level shifts for two- and three-dimensional bimetallic Pd_xCu_{1-x} and Pd_xAg_{1-x} alloys on Ru(0001). *Phys. Rev. B* **2005**, *72*, 075444.

58. Abrikosov, I. A.; Olovsson, W.; Johansson, B. Valence-Band Hybridization and Core Level Shifts in Random Ag-Pd Alloys. *Phys. Rev. Lett.* **2001**, *87*, 176403.

59. Simonov, P. A.; Moroz, E. M.; Chuvilin, A. L.; Kolomiichuk, V. N.; Boronin, A. I.; Likholobov, V. A. Influence of an interaction of $PdCl_2$ with carbon support on state and catalytic properties of Pd/C catalysts. In *Studies in Surface Science and Catalysis*; 1995; Vol. 91, pp. 977–987.

60. Álvarez-Montero, M. A.; Gómez-Sainero, L. M.; Martín-Martínez, M.; Heras, F.; Rodriguez, J. J. Hydrodechlorination of chloromethanes with Pd on activated carbon catalysts for the treatment of residual gas streams. *Appl. Catal. B Environ.* **2010**, *96*, 148–156.

61. Mahata, N.; Vishwanathan, V. Influence of Palladium Precursors on Structural Properties and Phenol Hydrogenation Characteristics of Supported Palladium Catalysts. *J. Catal.* **2000**, *196*, 262–270.

62. Martin-Martinez, M.; Gómez-Sainero, L. M.; Bedia, J.; Arevalo-Bastante, A.; Rodriguez, J. J. Enhanced activity of carbon-supported Pd–Pt catalysts in the hydrodechlorination of dichloromethane. *Appl. Catal. B Environ.* **2016**, *184*, 55–63.

63. Bonarowska, M.; Kaszkur, Z.; Karpiński, Z. Effect of silver on the catalytic hydrodechlorination of tetrachloromethane over silica-supported palladium-silver catalysts. *Recycl. Catal.* **2015**, *2*, 12–16.

64. Fung, S. Hydrogenolysis of methyl chloride on metals. *J. Catal.* **1987**, *103*, 220–223.

65. Heinrichs, B.; Delhez, P.; Schoebrechts, J. P.; Pirard, J. P. Palladium-silver sol-gel catalysts for selective hydrodechlorination of 1,2-dichloroethane into ethylene: I. Synthesis and characterization. *J. Catal.* **1997**, *172*, 322–335.

66. Xu, L.; Stangland, E. E.; Mavrikakis, M. Ethylene versus ethane: A DFT-based selectivity descriptor for efficient catalyst screening. *J. Catal.* **2018**, *362*, 18–24.

Tables and figures

Table 1. Characterization of the porous texture of the catalysts and carbon support.

Catalysts	A_{BET} ($m^2 \cdot g^{-1}$)	V_{micro} ($cm^3 \cdot g^{-1}$)	A_{EXT} ($m^2 \cdot g^{-1}$)	V_{pore} ($cm^3 \cdot g^{-1}$)
Carbon Merck	897	0.376	114	0.547
Ag/C	858	0.353	97	0.522
AgPdN/C	757	0.329	84	0.487
AgPdCl/C	823	0.341	86	0.507

Table 2. Surface and bulk contents of metallic species of the catalysts.

	Surface content (XPS)						Bulk content (TXRF)	
Catalysts	Ag (%)	Ag^0 (%)	Ag^+ (%)	Pd (%)	Pd^0 (%)	Pd^{n+} (%)	Ag (%)	Pd (%)
Ag/C	0.7	100	0	--	--	--	0.9	--
PdN/C	--	--	--	9.2	96	4	--	0.8
PdCl/C	--	--	--	1.1	57	43	--	0.9
AgPdN/C	1.7	35	65	7.5	91	9	0.9	0.9
AgPdCl/C	0.7	80	20	0.9	71	29	1.0	1.1

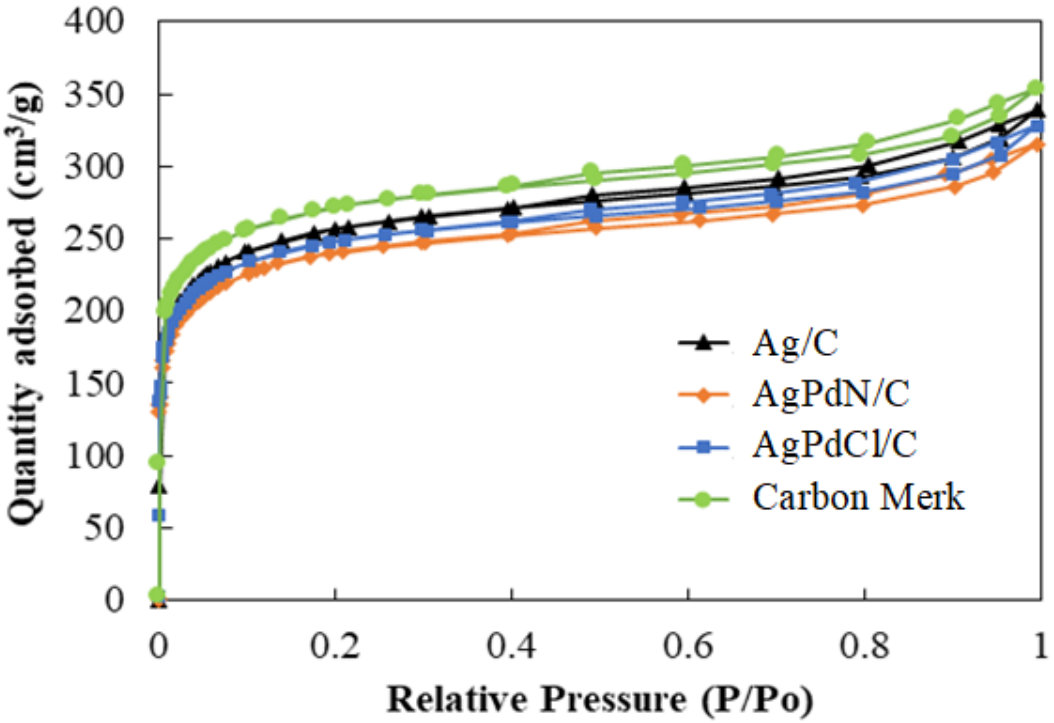

Figure 1. N_2 adsorption-desorption isotherms of the catalysts and carbon support at -196 ºC.

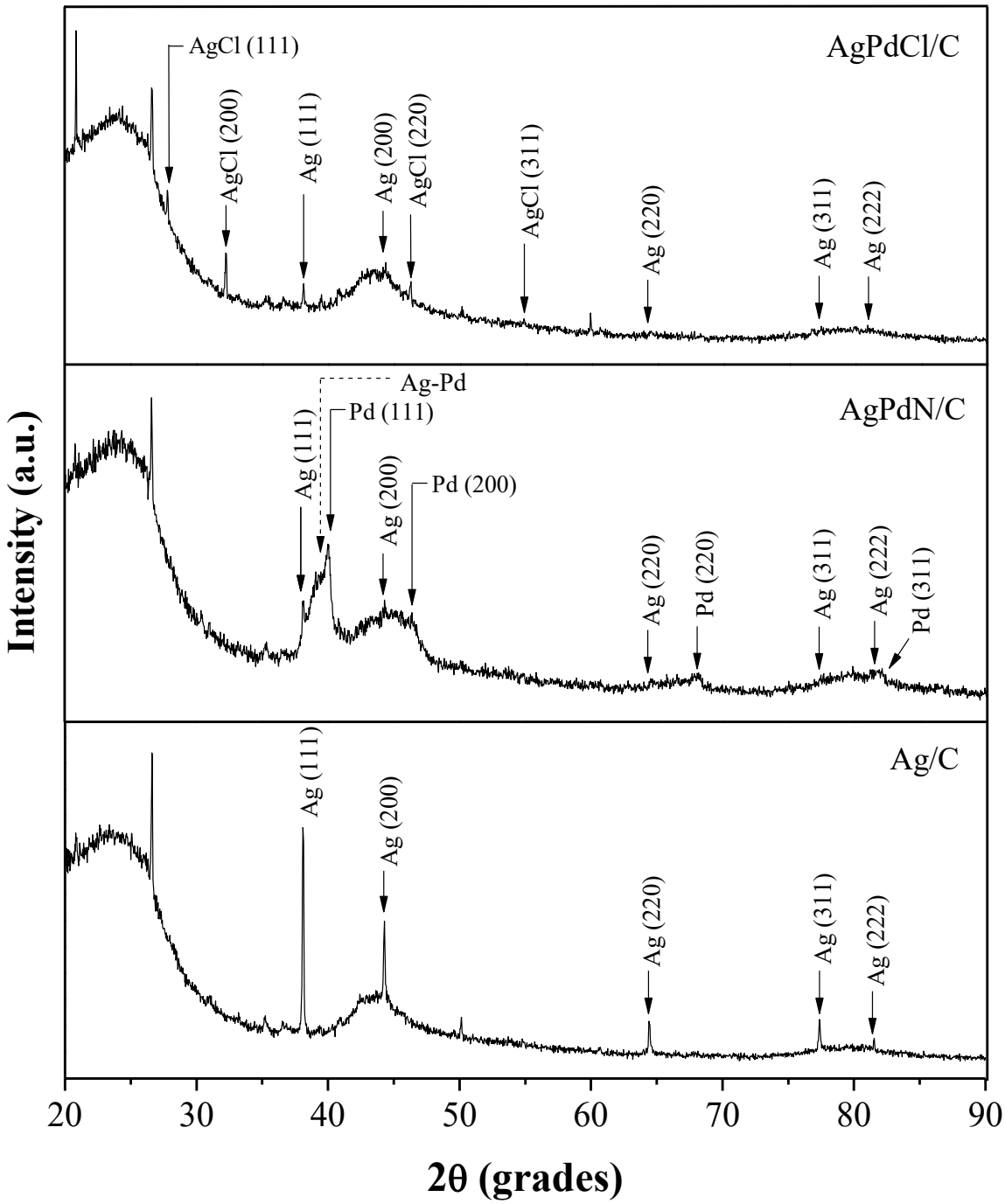

Figure 2. XRD patterns of the catalysts reduced at 250 ºC.

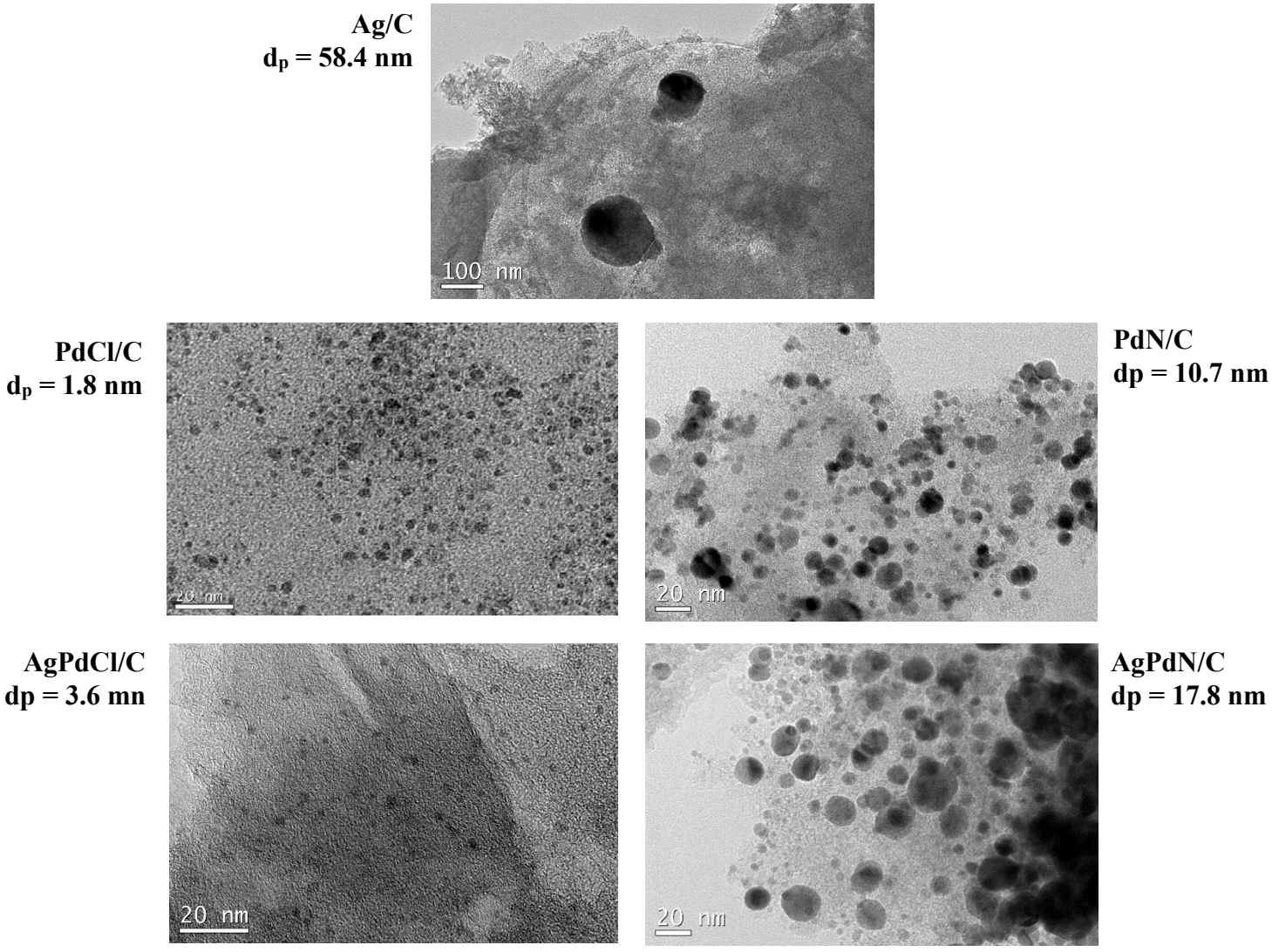

Figure 3. Representative TEM images and mean metal particle size (d_p) of the different catalysts.

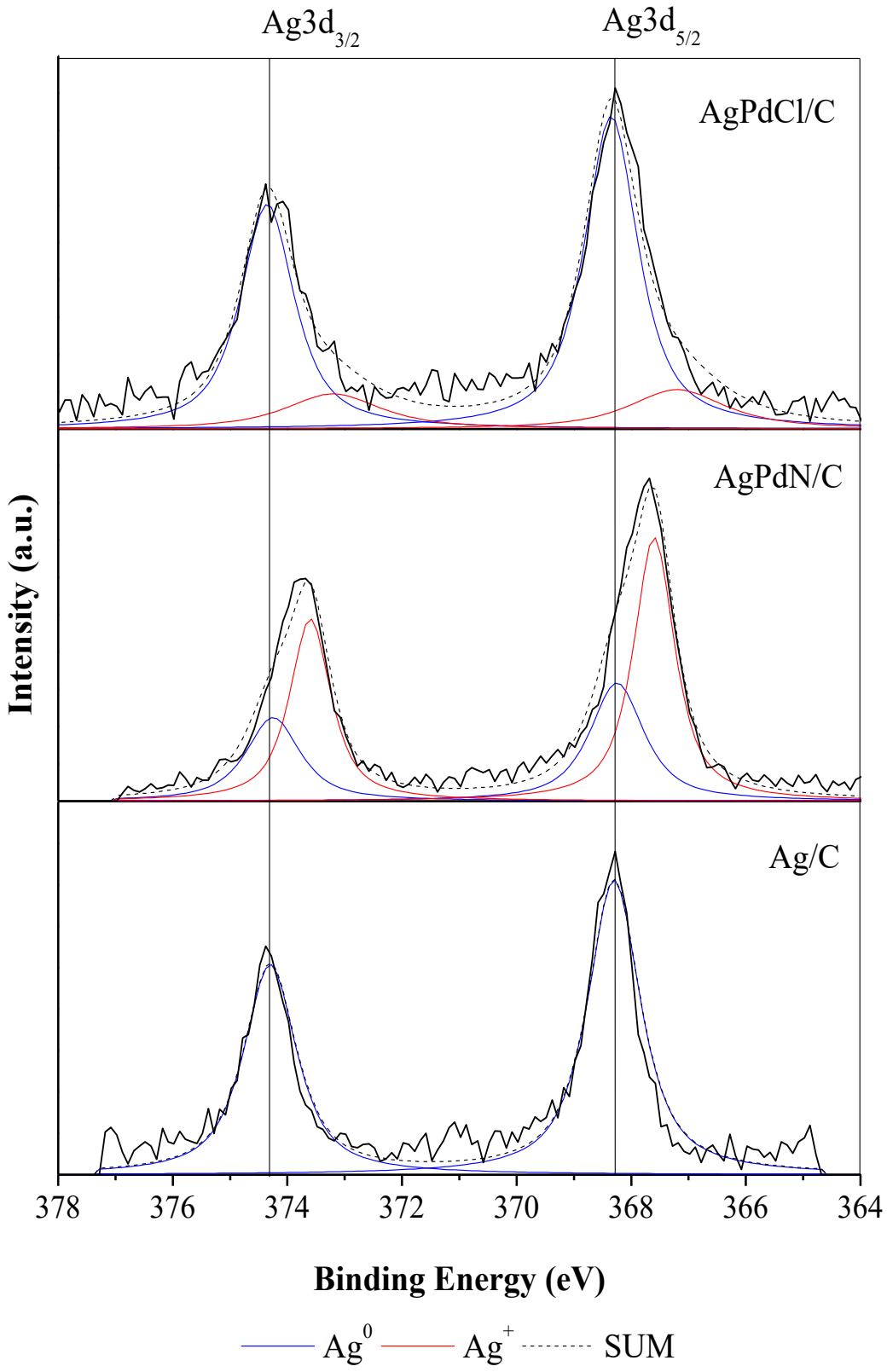

Figure 4. Ag 3d deconvoluted XPS profile of reduced catalysts.

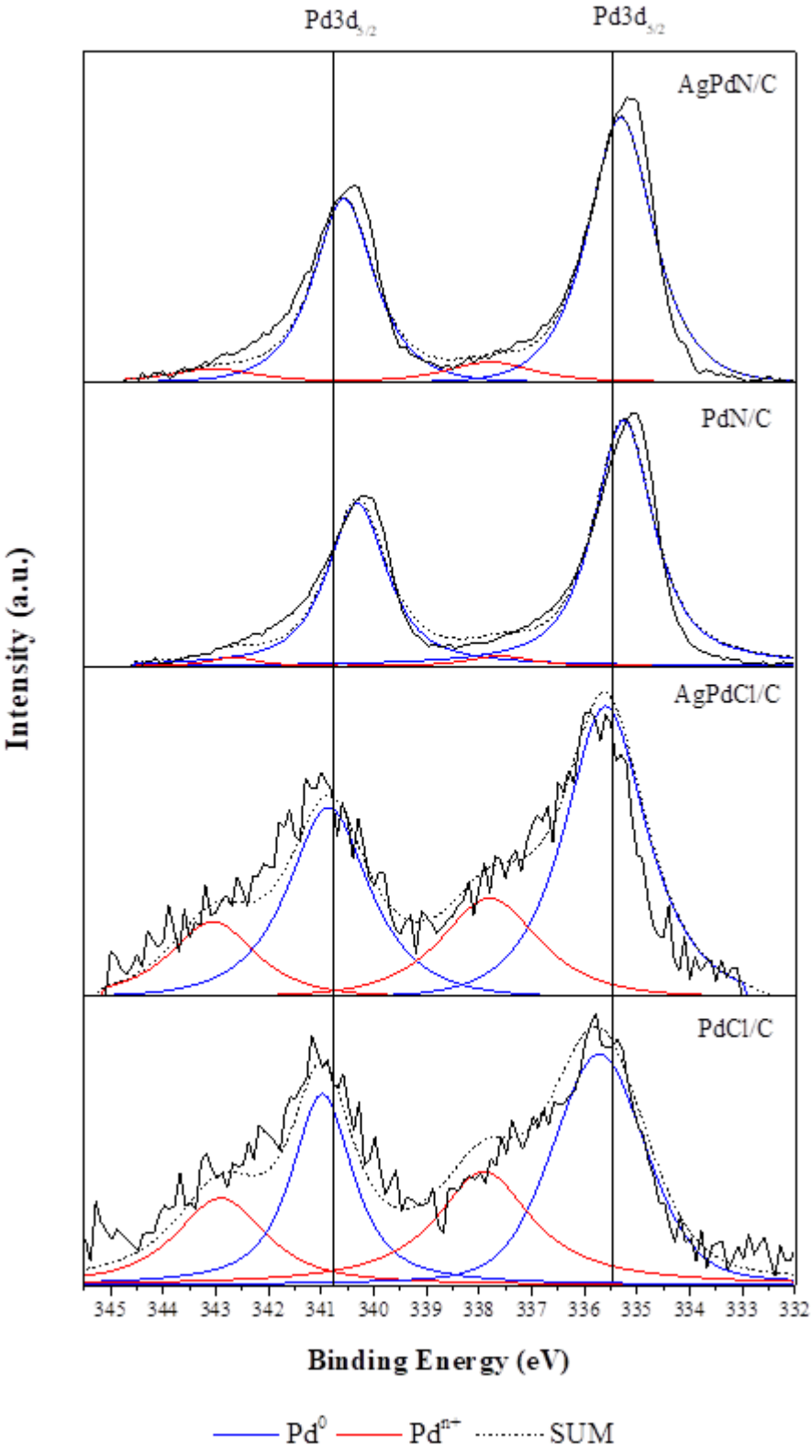

Figure 5. Pd 3d deconvoluted XPS profile of reduced catalysts.

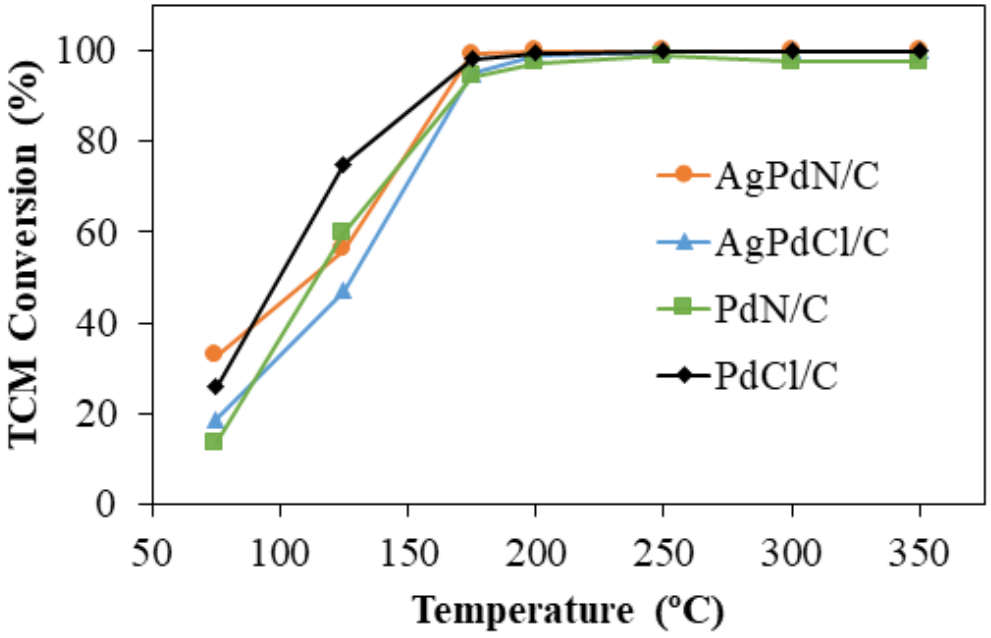

Figure 6. TCM conversion at different temperatures with the catalysts tested (τ= 0.8 kg·h·mol^{-1}, H_2/TCM molar ratio = 100).

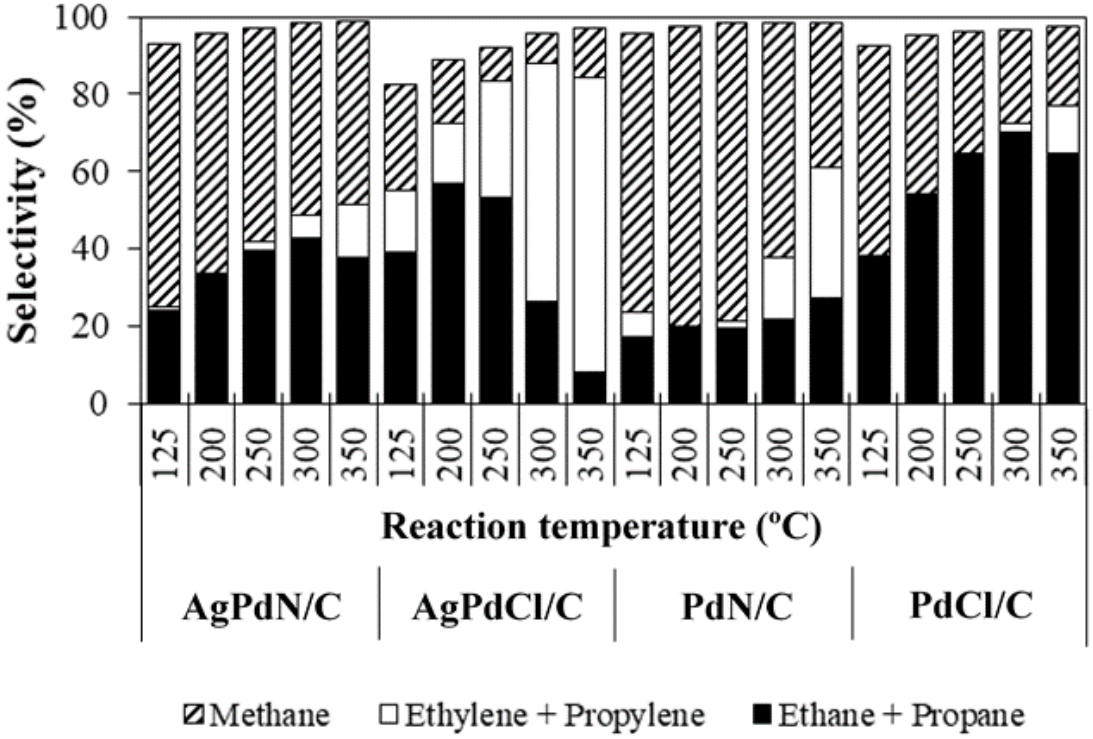

Figure 7. Selectivities to methane, olefins and other paraffins in the experiments of Figure 6.

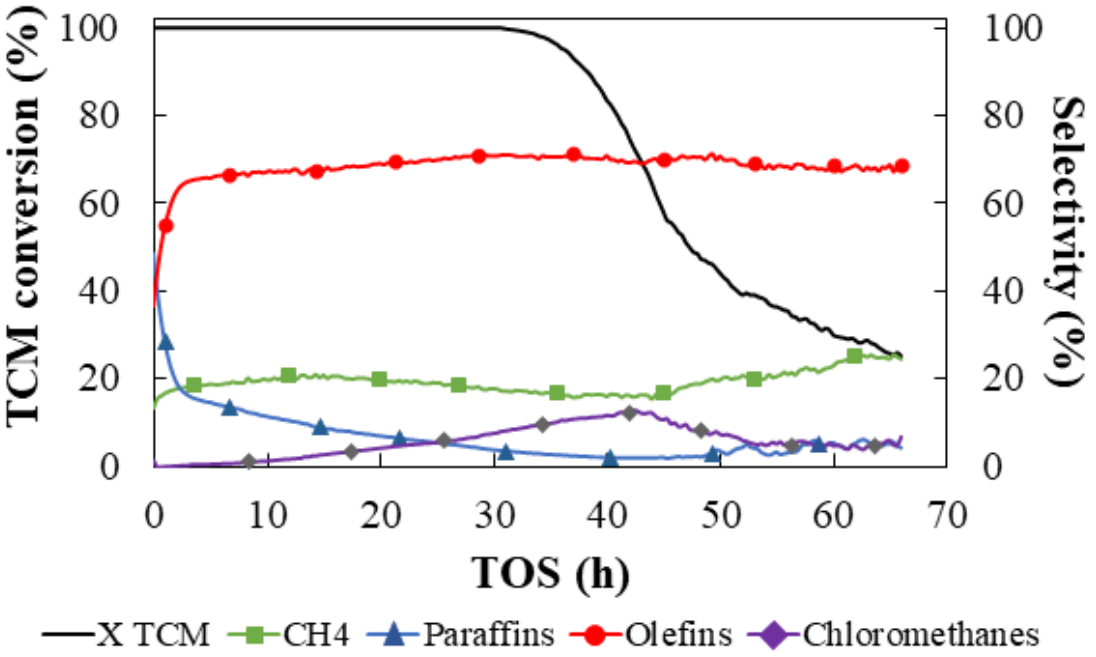

Figure 8. Evolution of TCM conversion and selectivities to reaction products upon time on stream at 350 ºC with the AgPdCl/C catalyst (τ= 0.8 kg·h·mol^{-1}, H_2/TCM molar ratio = 100).